

Review of optically active and nonlinear chiral metamaterials

Sean P. Rodrigues,^a Preston Cunha,^b Kaushik Kudtarkar,^b
Ercan M. Dede^{✉,a} and Shoufeng Lan^{✉b,c,*}

^aToyota Research Institute of North America, Ann Arbor, Michigan, United States

^bTexas A&M University, Department of Mechanical Engineering, College Station,
Texas, United States

^cTexas A&M University, Department of Materials Science and Engineering, College Station,
Texas, United States

Abstract. Advanced photonic nanostructures have enabled the maximization of synthetic chiroptic activities. The unique structuring of these building blocks has empowered chiral selective interactions with electromagnetic waves in plasmonic structures and dielectric media. Given the repertoire of optimized chiral surfaces in the literature and the ubiquity of chirality in the organic realm, the natural direction to consider is the operation of these devices in larger optical systems much like their chiral organic counterparts. Here, we recapitulate advances in active and nonlinear chiral metamaterials. Many of the results, such as the magneto-chiral anisotropy and third-harmonic Rayleigh scattering optical activity, are relatively unknown members of the more conventional family of tuning methodology and nonlinear processes. We believe that they are poised to play an instrumental role in designing advanced chiroptic systems for applications in biochemistry, valleytronics, spintronics, and chiral quantum optics. © 2022 *Society of Photo-Optical Instrumentation Engineers (SPIE)* [DOI: [10.1117/1.JNP.16.020901](https://doi.org/10.1117/1.JNP.16.020901)]

Keywords: metamaterials; chirality; nonlinear optics; nanophotonics.

Paper 22013V received Jan. 24, 2022; accepted for publication Apr. 1, 2022; published online Apr. 22, 2022.

1 Introduction

Chiral electromagnetism, often referred to as optical activity (OA), has two main properties that describe the way a wave interacts with a given chiral medium. The first is optical rotatory dispersion (ORD) in which the polarization of a wave is rotated as it passes through a chiral medium. The second is circular dichroism (CD) dispersion, which describes the asymmetric absorption of light upon incidence with a chiral medium.¹⁻³ The experimental discovery of ORD was realized by Louis Pasteur in 1856 when he noticed that pure crystalized forms of (\pm) lactic acid were able to rotate the polarization of a linearly polarized light wave.^{4,5} To this day, this optical description of chirality is used as a characterization system to classify molecular behavior. For instance, D-glucose is naturally occurring in organic life and is capable of being broken down into an energetic form for the human body, while L-glucose is simply passed through the digestive system unutilized by the metabolism; even though both forms of glucose retain the same molecular components, their conformation (not configuration) is slightly different. This alternate conformation arises from the tetrahedral nature of carbon; the bonding angles of these atoms induce alternate forms even if the atoms are connected in the same delineation in both molecules. This naturally occurring asymmetry requires extreme care in the asymmetric synthesis of chemicals and pharmaceuticals. Research in this field has led to Nobel prizes in 2001 and 2021.⁶⁻⁸ However, the ability to measure these optical signals in small samples of organic molecules is often difficult due to their OA appearing in the UV region and the variation being often on the order of millidegrees. Despite improvements in measurement components, such as lasers and photodetectors, the critical functionality of how to measure chiral OA from organic materials has not changed much since the inception of these measurements systems.

*Address all correspondence to Shoufeng Lan, shoufeng@tamu.edu

For instance, measurements of the first systematic observation of cotton effects stemming from protein conformations in 1966 rely on polarimeters that are similar to what we use today.^{9–12}

This introduction, largely descriptive of the realm outside chiral metamaterials, gives insight into the necessity that has driven the exploration of artificially produced OA. Some of these important objectives include determining if large chiral OA can be synthetically achieved, if the sensitivity of optically active signals can be increased, and how chiral-selective behavior can be implemented in electromagnetic applications such as its operative counterpart in biology. These directives have been extensively researched over the past several years, leading to significant advancements through the utilization of chiral metamaterials. Here, we provide demonstrative references for the above objectives using chiral metamaterials, respectively, for OA,^{13–22} chiral-selectivity,^{23–25} and applications.^{26–28} In this review, the term “metamaterials” describes the structuring of two or more materials with different refractive indices to form a local unit cell. This local unit cell is then periodically repeated to form a larger global material, which has an effective refractive index. Typically, optical metamaterials have a unit cell size that is on the order of or smaller than the wavelength of the radiation of interest.²⁹ In particular, chiral metamaterials utilize structural asymmetry at the local level to induce chiroptical responses. Chiral metamaterials created from plasmonic materials, such as gold, silver, and titanium, have been utilized to create strong chiral resonances in the visible and near-infrared regime. Several papers describe how to create strong chirally resonant optical devices by understanding the interplay of the polarization of incident light with the three-dimensional (3D) design of the optical structure.³⁰ While the advancement of nano-optics artificial chirality has grown significantly in the past several years, it should be noted that the use of artificial materials to manipulate the polarization of electromagnetic waves dates back to the 1890s when Bose observed that jute rope could induce a rotation on the polarization of a millimeter wave.³¹

In this review, the authors highlight recent progress on active and nonlinear chiroptical metamaterials. In particular, we refer to “active” as the dynamic response of a metamaterial to an external stimulus that modifies the output of the light that has been incident on the metamaterial. The goal of this review is to focus on the temporal modulation of these materials rather than the fixed tailorable response. In the past 5 years, there has been a surge of research on the modification of the local or effective refractive index of media, thus enabling the research of a diverse set of switchable or temporally tailorable optical properties. Many paths of research that are related, but out of the scope of this review, include a review on multidimensional nanoscopic chiral optics,³² a review on chiral quantum optics,³³ and reviews on active metamaterial structures in general.^{34,35}

Before discussing the role of active photonics in chiral artificial media, a review of definitions and terms is presented. CD is defined as the difference in absorption between left circularly polarized (LCP) and right circularly polarized (RCP) waves, $CD = A_{RCP} - A_{LCP}$. However, as many optical metamaterials often demonstrate very low values for reflectance, values of transmission are often used in place of absorption. It should be noted that CD is intimately related to optical rotation dispersion via the Kramers Kronig relations.^{36,37} Also, it is important to note that a robust way to understand the Jones matrix of a material is to understand the polarization and intensity of light prior to and after incidence onto the structure; to this end, Stokes polarimetry can provide a detailed analysis of the light and thus its interaction with the material via Mueller calculus.³⁸ Given the Stokes vectors, the handedness of the input and output waves can be depicted on a Poincare sphere for analysis. Finally, although CD is a definitive method to realize linear optical chirality, many researchers have found new and exotic ways to usurp this property through the emission of quantum dots (QDs), the use of photophores, and the implementation of nonlinear tensors to create extractable, larger chiral responses, many of which are discussed in more detail below.

2 Active Chiral Metamaterials

As we understand from Sec. 1, the chiroptical signal generated by chiral metamaterials can largely surpass that of its organic counterparts due to the strong coupling between electric and magnetic fields in the chiral nanostructures. With this understanding in mind, one could envision many practical applications from sensing to communications that could result from studying how

external stimuli can modify the effective chiral features of the material, including the spectral location and magnitude.^{39–41} To reach this step, researchers have learned how to manipulate and probe the chirality of these metamaterials actively.^{42–44} To this end, the study of active photonic structures has employed many methods, including optical, electrical, and mechanical means. In Sec. 2, the review of the active structures is categorized broadly into three categories, namely, active chiral metamaterials with static structures for tailored coupling efficiency, active chiral metamaterials with reconfigurable structures for control of chirality, and externally modulated chiral systems.

2.1 Active Chiral Metamaterials with Static Structures

For practical reasons, active chiral metamaterials with static structures are desirable. To change the coupling strength between electric and magnetic fields while keeping the structures intact, researchers use active constituting materials with properties that change with external stimuli. In the electromagnetic region, these material properties are the permittivity, permeability, or refractive index. It is possible that the electromagnetic properties of a given material are sensitive to external stimuli, such as a secondary optical wave, magnetic flux, a thermal flux, etc. As chiral metamaterials are often composites of two or more materials, the effective index determined by the structuring of these materials has more opportunities to modify light than a standard bulk medium. For this reason, active chiral metamaterials can be created with static devices because the electromagnetic coupling strength that signifies the strength of chirality can be modulated with and without the stimuli. As an example, some phase-changing materials such as VO_2 can change from a metallic state to a dielectric state with electromagnetic properties that are dramatically different upon the application of heat. As a result, by employing active materials as constituents in artificial chiral structures, researchers have developed various methods to manipulate chirality correspondingly.

2.1.1 Optically active chiral metamaterials

Among the variety of active stimuli to manipulate metamaterials, secondary optical sources are of great interest as they often are associated with high-speed modulation depths. The typical materials used for optical modulation are semiconductors because the conductivity changes dramatically with optical pumping at an energy higher than the bandgap (Fig. 1). In the terahertz (THz) regime, Kanda et al.⁴⁵ switched the chirality of their material on and off with optical pumping. This is achieved using the distribution of photo-generated carriers in a silicon layer together in

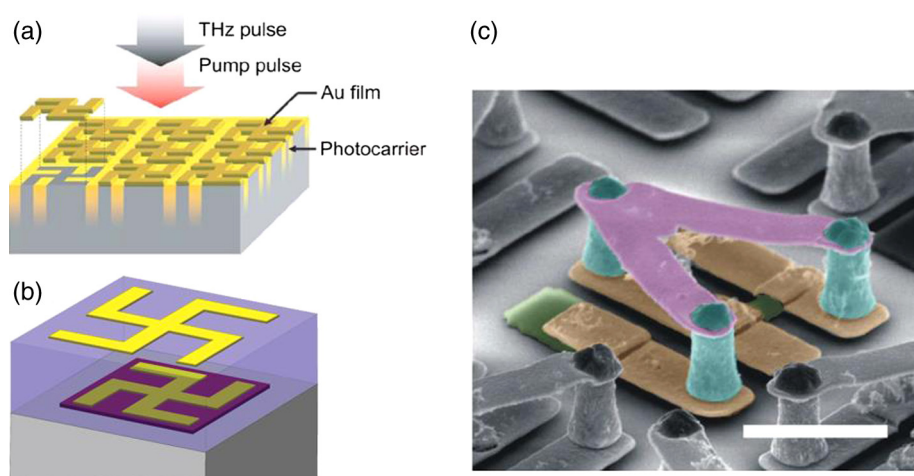


Fig. 1 Static optically active chiral metamaterials with 3D shaped nanostructures. The photoexcited carriers in semiconductors change the electromagnetic properties dramatically and hence are used as optically active constitutive materials for chiral metamaterials. The devices contain (a) a single-layer,⁴⁵ (b) a double-layer gammadion-shaped chiral metallic structure,⁴⁶ and (c) a sophisticated V-shaped geometry bolstered by pillars (scale bar is 10 μm).⁴⁷

combination with a chiral gammadion-shaped metallic nano-structure. The intrinsic chirality in the single-layer metallic structures is too weak to be seen by the THz waves, but the authors successfully managed this by extending the thickness with the distribution of photo-generated carriers to the thick silicon substrate. The polarization rotation angle is <1 deg at the resonant frequency. Using a bilayer conjugated metallic structure together with a thin intrinsic silicon layer, Zhou et al.⁴⁶ further enlarged the rotation angle to tens of degrees. With a judicious design, Zhang et al.⁴⁷ introduced a metamolecule monolayer that flips the ellipticity of the chiral metamaterial. Such an electromagnetic effect is much stronger than that of naturally available molecules. This is promising for creating a compact polarizer with dynamic control of the polarization of light.

2.1.2 Thermally active chiral metamaterials

Compared with optical methods, thermal activation methods are usually much slower, occurring on a timescale of seconds for large bulk materials. This longer thermal time constant for activation is related to the diffusion of heat required to articulate sufficient changes in the bulk properties of the thermally active materials. However, at the nanoscale, these heat-induced material property changes may occur more rapidly. The most vastly available thermally modulated materials are phase change materials, which have electromagnetic properties that change dramatically upon the application of heat. The heat breaks the chemical bonds in the material and changes the phase of the material from crystalline to amorphous. More importantly, when the temperature cools, the amorphous phase changes back to the more stable crystalline phase. The reversible characteristics of thermally transduced phase change materials opens a slew of real-world applications. One thing of note is that phase change materials can be controlled not only by heat but also by other methods such as light and electricity. In this section, however, we limit ourselves to the discussion of thermal methods. An example of a phase change material is $\text{Ge}_3\text{Sb}_2\text{Te}_6$ (GST-326). By applying a thermal gradient to the design of a chiral metamaterial that utilizes this phase change materials, researchers have been able to spectrally tune the resonant wavelength of the active chiral metamaterial.⁴⁸ The spectral shift is due to the dielectric constant change between amorphous and crystalline GST-326 states in the studied mid-infrared (MIR) spectral region. Subsequently, by utilizing this effect in combination with a passive chiral bias-type layer, the authors were able to switch the sign of the CD signal in the MIR [Fig. 2(a)]. As CD is measured on a scale ranging between -1 and $+1$, being able to switch the overall handedness of the material, and thus the chiroptical signal from negative to positive, or vice versa, is significant in terms of modulation depth. One way to extend the resonant wavelengths to other spectral regions, such as visible, near-infrared (NIR), or THz, is to use different phase change materials.⁵⁰ Utilizing a slightly different phase change material such as $\text{Ge}_2\text{Sb}_2\text{Te}_5$ (GST), researchers have been able to reversibly tune a glass chalcogen material at nanosecond or less timescales. The phase change nanomaterial has a helical structure, as shown in Fig. 2(b); the width of the rod of the helix is 15 nm, with a radius of 22.5 nm and a pitch of 45 nm. The nanostructures are created using a glancing angle deposition technique, and the metamaterial switches from exhibiting large OA to weak OA with demonstrated dynamic switching over 50,000 cycles.⁴⁹

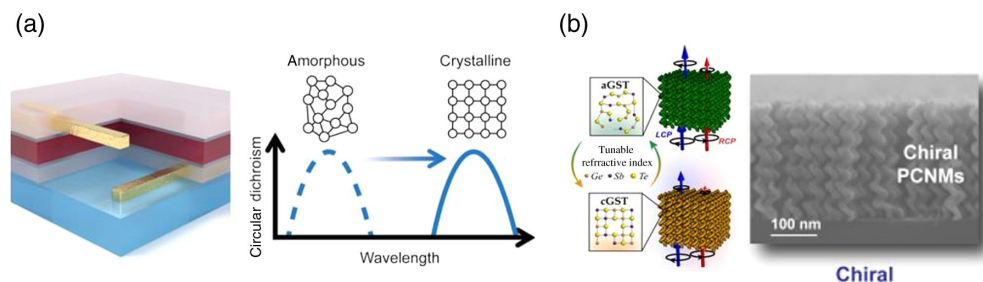


Fig. 2 Thermally active chiral metamaterials. (a) The thermally active phase change material is GST-326, which changes from a crystalline to amorphous state when applying heat.⁴⁸ (b) A phase change nanomaterial also made of GST is capable of increasing/decreasing chirality by an external heat stimulus and shows no change in properties over 50,000 cycles.⁴⁹

2.1.3 Electrically active chiral metamaterials

An alternate method for the direct tuning of chiral metamaterials is to use electrical control, which is attractive because of the compatibility with existing information processing systems, telecommunications, and so on. Unfortunately, electrical tuning of CD and OA is extremely challenging because the electrical doping level is hardly comparable with the total density of states in bulk materials. However, this scenario is dramatically different in two-dimensional (2D) materials. By integrating 2D graphene in a chiral metamaterial, Kim et al.⁵¹ tuned the transmission of an RCP light while maintaining the transmission constant for the other circular polarization. In this way, the authors were able to tune the CD by applying a gate voltage. The authors further showed that they could also tune the plane of linearly polarized light while the linear polarization state maintains its linearity in the same device. The nuance here is that most conventional chiral optical systems modify a linearly polarized wave into an elliptically polarized wave. Maintaining the linear polarization is a property that is typically observed in birefringent media. The benefit from the electric control of polarization is that the 2D material concept may lead to various applications such as a compact active polarization modulator for telecommunications and imaging devices. Similar demonstrations of graphene-embedded, THz, chiral-modulation devices have also been demonstrated.^{52,53}

2.1.4 Magnetically active chiral metamaterials

Here, the magneto-chiroptical properties of metamaterials are investigated. Naturally, to achieve a modulation depth in the optical spectrum via magnetic tuning, the effective refractive index of the metamaterial must be reliant on a magnetically tunable material. To this end, the goal is to implement a type of interaction that is typically observed in chiral liquids known as the Cotton-Mouton effect or, in more general substances, as the Faraday effect. To demonstrate this magnetic tunability, researchers introduced cobalt into the fabrication of a layered silver nanohole array, thus demonstrating a change in the modulation depth of 0.035 deg using this chiral metamaterial. The interplay between the two materials and the geometrical structure of the hole array enables stronger magnetic CD.⁵⁴ Beyond the first-order Faraday effect that is linearly proportional to the magnetic field, magnetism also sustains higher-order interactions with chirality stemming from their shared nature of an axial vector. One prominent example is the magneto-chiral effect, which is proportional to the inner product of the magnetic field and the wavevector.⁵⁵ This relatively unknown degree of freedom provides a new route for exotic functionalities that are generally not achievable solely by magnetism or chirality. These functionalities include enantiomeric excess in photochemical reactions and the separation of racemic mixtures. Though it is omnipresent and responds to photons, electrons, and phonons, the observed magneto-chiral anisotropy is on the order of 0.1%. By judiciously arranging gold nanoparticles on gold/cobalt magnetic multilayers as shown in Fig. 3, Armelles et al.⁵⁶ obtained a magneto-chiral response to surface plasmons with a magneto-chiral anisotropy of around 1%. Very recently, Lan et al.⁵⁷ reported the first observation of a magneto-chiral response to excitons with a record-high magneto-chiral anisotropy of ~4% in twisted van der Waals crystals. Moreover, by coupling to the valleys in the electronic band

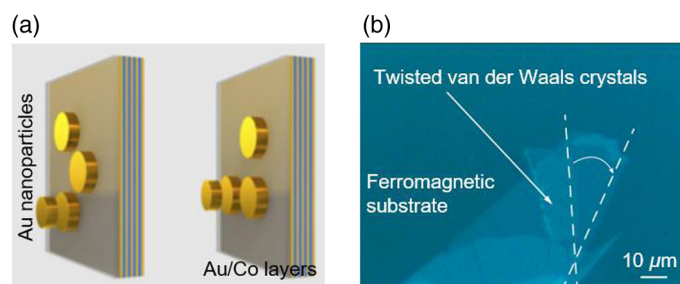


Fig. 3 Magnetically active chiral metamaterials through the magneto-chiral effect. (a) By placing purposely arranged chiral plasmonic gold nanoparticles on gold/cobalt magnetic multilayers, the magneto-chiral anisotropy is around 1%.⁵⁶ (b) Twisted van der Waals crystals on a ferromagnetic substrate increase the magneto-chiral anisotropy to 4%.⁵⁷

structure, such metamaterials may find applications in the surging field of valleytronics.⁵⁸ This technology may also contribute to recent electron quantum metamaterials using van der Waals crystals as building blocks.⁵⁹

2.2 Active Chiral Metamaterials with Reconfigurable Structures

Intuitive thinking to tune the coupling between electric and magnetic fields and hence the chirality is to reconfigure the structures of chiral metamaterials. Imagine that, as the distance between metamolecules, the thickness of layers, or the geometry of structures changes, the field distribution, as well as the coupling, must change accordingly. Indeed, with external stimuli giving rise to a strong enough force, researchers have demonstrated various active chiral metamaterials. The challenge lies in finding the right sources and materials for providing the force to introduce structural changes. Those sources can either be mechanical, chemical, or biological. Due to limited space, focus is given to the review of experimental works in this section.

2.2.1 Mechanically reconfigurable chiral metamaterials

Photoexcitation for chiral metamaterials with static structures can switch the handedness. On the other hand, static structures with active materials lack enantiomeric symmetry, which results in asymmetric OA spectra. Therefore, there is a considerable need for an active chiral metamaterial with the switching capability and symmetrical OA spectral shapes between the different handedness structures. Mechanically reconfigurable chiral metamaterials fulfill this need.

In this section, we review several mechanically reconfigurable structures that are actuated by various stimuli. In the THz region, Kan et al. proposed and experimentally demonstrated a micro electro mechanical systems (MEMS) chiral metamaterial facilitated by a deformable 3D chiral structure.^{60–62} Later, these same springs were deformed via physical movement after having the center of the spirals glued.⁶³ The directional switching of the pneumatic and/or electrostatic actuation enabled an OA polarity reversal while maintaining a constant energy transmittance and spectral shape, thus achieving enantiomeric handedness switching. Also, in the THz regime, researchers demonstrated birefringence-free tunability with pneumatically tuned helices rather than the spirals previously discussed.

Figure 4 shows a few more depictions of electrically controlled modifications of the reconfigurable metamaterial. Figure 4(a) shows active control of CD by nanoelectromechanically tunable doped silicon interdigitated structures. The device depicts distinct wavelength resonance shifts, thus enabling strong shifts in CD at specific wavelengths.⁶⁴ In another example, a gold film metamaterial is fabricated on a substrate. By applying a voltage, the metamaterial goes from a 2D thin film to a 3D chiral nanostructure through nano-kirigami folding.⁶⁵ Finally, Fig. 4(c) provides mechanically folded tuning angles as well as and electrical tuning of the Fermi energy level of graphene. This paper also provides a set of videos depicting the folding animations and their respective transmission plots for both left- and right-handed structures.⁵³

Mechanical tuning of OA has also been observed by strategically designing chiral metamaterials on polydimethylsiloxane (PDMS) substrates.⁶⁶ In a similar vein, researchers utilized glancing angular deposition on polystyrene nanosphere arrays to create hollow nanoshells and hollow nanovolcano film arrays; these structures are then integrated into PDMS substrates that have shown mechanical deformation to achieve active CD of the composite structure. PDMS, hydrogels, and other curved plastics are highly desirable for medical sensing designs. Using the design described, researchers were able to create reference tables to signify water content absorption of hydrogels.⁶⁷ This kind of deposition process, also known as shadow lithography, has been studied at length by the Zhao group for the creation of chiral nanostructures^{68–70} and other groups for other metamaterial structures.⁷¹

2.2.2 Biochemically reconfigurable chiral metamaterials

In this section, we review chiral metamaterials that have been modified to have responses to biochemical or chemical inputs. By transducing these chemical inputs into forces or chemical reactions, the metamaterials have dynamic responses that are visible in their chirOA. As a first

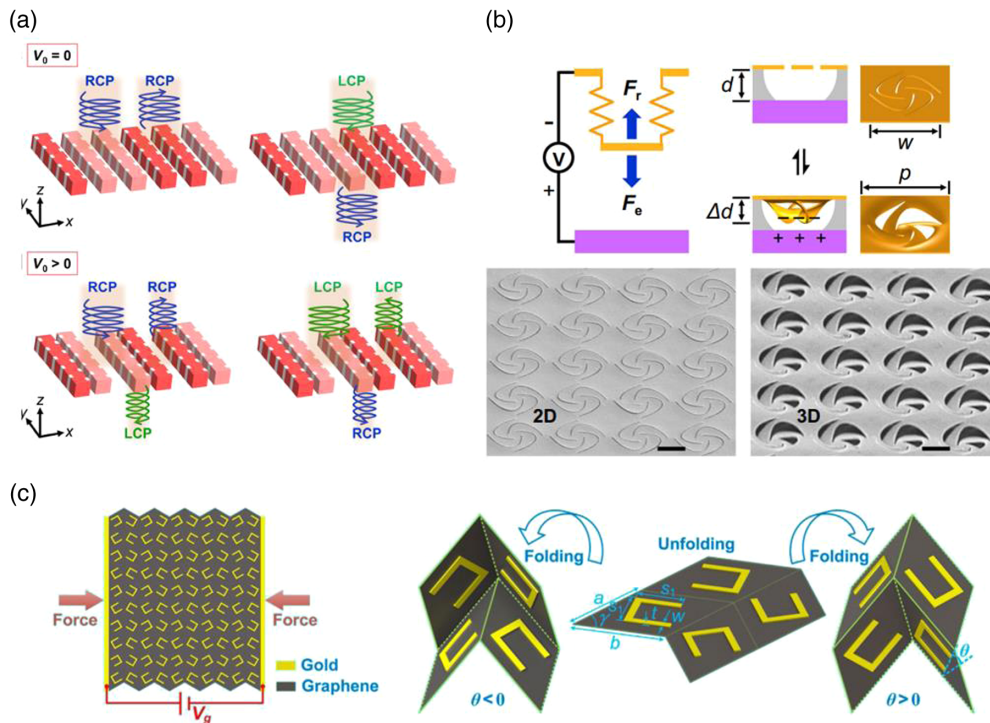


Fig. 4 Electrically transduced mechanically reconfigurable metamaterials. (a) Interdigitated electrodes are patterned in metal. The electrodes are pulled in toward each other to instill either a right-handed or left-handed chiral metamaterial structure.⁶⁴ (b) A gold metamaterial membrane is bolstered by silicon dioxide pillars that sit on a silicon wafer. The silicon and the gold act as electrodes to implement the reconfigurable structure from a 2D orientation to a 3D orientation.⁶⁵ (c) Here, this G-mori type metamaterial structure shows both mechanically induced folding and electrical tuning of the Fermi level of the graphene substrate.⁵³

example, Kuzyk et al.⁷² used deoxyribonucleic acid (DNA) as a construction material to organize individual plasmonic nanoparticles to drive the metamolecule to distinct conformational states. Despite the demonstration of mechanically reconfigurable individual chiral metamolecules with DNA, active regulation of chirality with a collective motion of metamolecules, particularly in the visible spectral region, still faces significant challenges. Duan et al.⁷³ demonstrated a new class of hybrid plasmonic metamolecules composed of magnesium and gold nanoparticles. The chirality from such plasmonic metamolecules can be dynamically controlled by hydrogen in real-time. In this case, although gold structures did not change, we classify them as reconfigurable chiral metamaterials because part of the structures switches forms between MgH_2 and Mg , interchangeably. The researchers use a silk layer as a spacer between two twisted gold hole arrays, or so-called Moiré patterns, to demonstrate tunable chirality of chiral metamaterials in the visible region.⁷⁴ The silk spacer changes the thickness with chemical solvents and hence changes the coupling between the electric and magnetic of the chiral metamaterials. They further used this biochemically active chiral metamaterial as a sensor to detect solvent impurity of solutions [Fig. 5].

2.3 Modulated Chiral Systems

Also worth discussing in this review are modulated chiral systems, in which modulation occurs near or around the chiral metamaterial but does not directly impact the refractive index of the metamaterial itself. Examples of this are shown in Fig. 6. In one case, a liquid crystal is placed on top of an L-shaped chiral metamaterial. In this situation, the liquid crystal is able to locally alter the polarization of the incident light, thereby creating an active optical system for spin-selective light absorption in the near-infrared regime.⁷⁵ In a similar vein, liquid crystals have been used

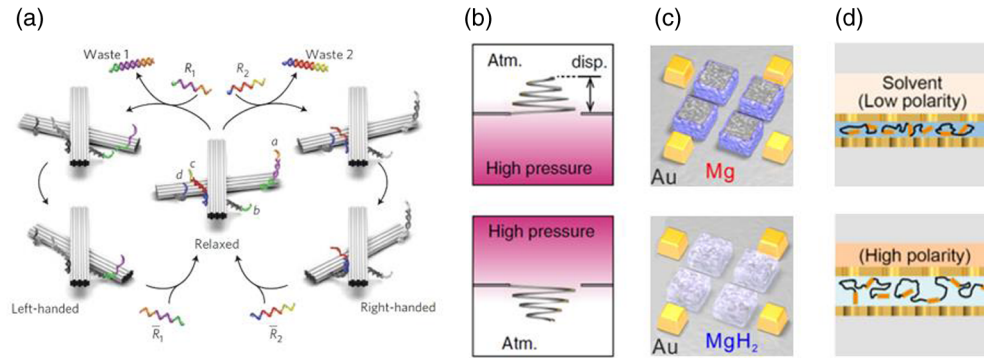


Fig. 5 Reconfigurable chiral metamaterials. The structures are reconfigurable with (a) DNA,⁷² (b) pressure,⁶⁰ (c) hydrogen,⁷³ and (d) solvents,⁷⁴ respectively. When the structures and geometry changes, the coupling of electric and magnetic fields, as well as chirality of the chiral metamaterials, changes accordingly.

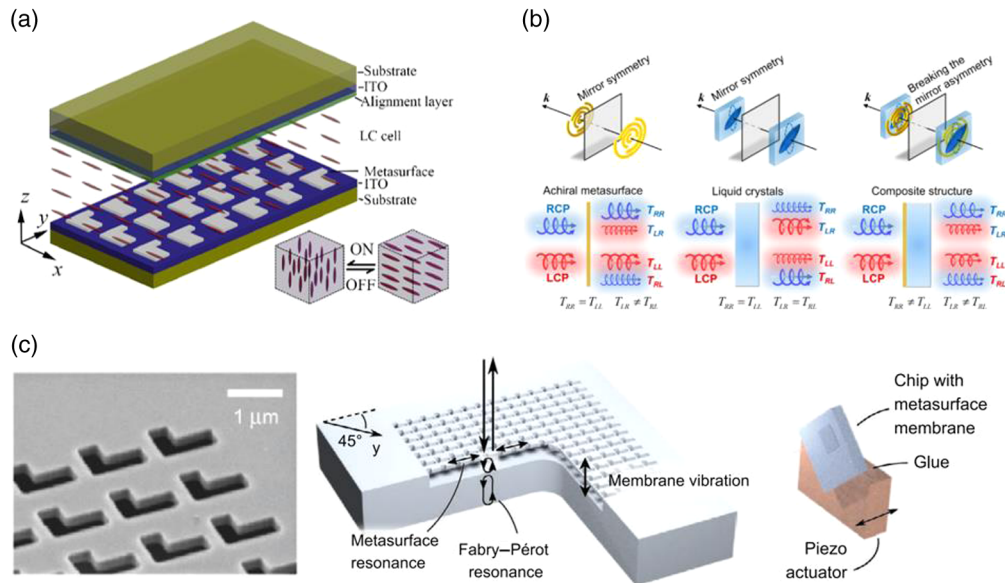


Fig. 6 Externally modulated chiral systems. Liquid crystals placed adjacent to metamaterial structures provide optical systems (a) with spin-selective absorption in the NIR⁷⁵ and (b) that break axial symmetry in the THz regime.⁷⁶ (c) A GaAs metamaterial membrane is vibrated, while spin selective optical forces are imparted onto the membrane thanks to the handedness of the metamaterial.⁷⁷

externally to realize metamaterials in the THz regime, as shown in Fig. 6(b).⁷⁶ In this case, the liquid crystal axis is spatially on the order of the metamaterial, thereby modifying the axial symmetry of the device. Another example of externally modulated chiral systems is that shown Fig. 6(c). Here, the structure is mechanically modulated by a piezoelectric actuator. The L-shaped metamaterial is created in a GaAs membrane structure. The structure exhibits 3D chirality due to its Fabry-Pérot resonances between the membrane-substrate optical paths. The optomechanical coupling is then investigated; by vibrating the membrane and imparting changes to the phase, the intensity and polarization of light is controlled. The membrane oscillations are achieved by piezoelectric actuation.⁷⁷ The device has a unique feedback effect in which the polarization state of the imparted photons shifts the resonant frequency of the mechanical resonator through an optothermal spring effect. Moreover, this shift in the resonant frequency is spin-selective thanks to the directionality of the circularly polarized light.

3 Nonlinear Chiral Metamaterials

Light-matter interactions in traditional chiral materials manifest in magnetic dipolar interactions, which are usually much weaker than the electric dipolar interactions that dominate the linear optical phenomena such as transmission, reflection, and absorption. Consequently, chiroptical properties, including CD and ORD, are typically more than two-order smaller than linear optical properties such as scattering. While CD designates distinct absorptions from incident LCP and RCP light, ORD designates the polarization rotating ability of a chiral material. Nonlinear optical interactions such as second-harmonic generation (SHG) and sum-frequency generation, however, allow for electric dipolar interactions in media without inversion symmetry. Therefore, the nonlinear chiral responses are comparable with achiral nonlinear responses in chiral materials. For this reason, nonlinear, optical excitation tools such as SHG-CD and two-photon luminescence (TPL) CD have been developed to better identify and realize features unrecognized under linear excitation conditions.^{78–81} Chiral metamaterials have proven to be powerful nonlinear optical tools in the investigation of chiroptical properties with high sensitivity.⁸²

3.1 Second-Order Nonlinear Chiroptical Processes

The simplest but basic nonlinear optical process is SHG, in which two photons at the same frequency generate a new photon with the frequency doubled in nonlinear media. The SHG is sensitive to symmetry breaking and surface conditions; therefore, it has been a critical nonlinear optical tool for investigating chiral metamaterials. Valev et al.⁸³ used chiral metamaterials with the Slavic shape and its mirror-image to unambiguously observe the large distinct SHG from LCP and RCP light; see Fig. 7, the SHG-CD. The authors attributed the large SHG-CD to the superchiral field of hotspots.⁸⁵ The authors also showed that, whereas chiroptical properties in the linear optical regime are reciprocal, in the nonlinear regime these effects can be non-reciprocal. Meanwhile, as shown in Fig. 7, Rodrigues et al.⁸⁶ introduced a twisted-arc chiral metamaterial that has an SHG-CD of ~ 2 , the largest value on the chiral-SHG scale. More interestingly, by embedding QDs into the twisted-arc chiral metamaterial, the same group observed a largely enhanced TPL-CD, another second-order nonlinear chiroptical phenomenon.²⁴

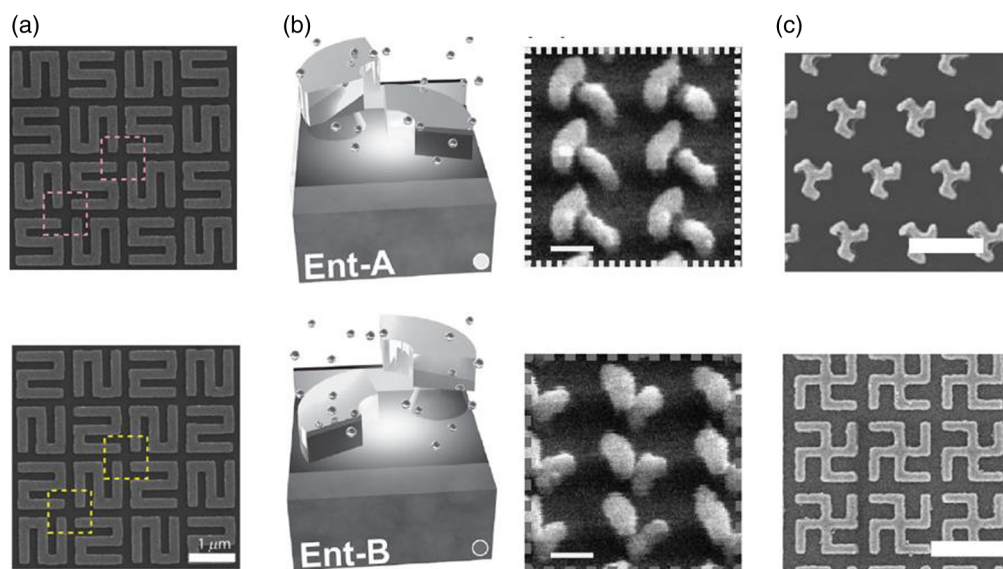


Fig. 7 Nonlinear chiral metamaterials. Nonlinear chiroptical properties, including SHG-CD and THG-CD, are observed in various geometries, such as (a) the rotating-S,⁸³ (b) twisted-arcs,²⁴ and (c) trisceli- and gammadion-type structures.⁸⁴

3.2 Third-Order Nonlinear Chiroptical Processes

As described previously, optical properties are generally associated with refractive index of a medium. When the refractive index changes with the intensity of the light, it generates a nonlinear optical phenomenon that typically relates to the third-order nonlinearity. In chiral metamaterials, such third-order nonlinearity leads to a novel phenomenon called nonlinear OA. A comprehensive study on the third-harmonic CD of bilayer metamaterials is provided by Gui et al.,⁸⁷ in which they utilized a Born–Kuhn analog to understand the chirality of nanorods arranged in C4 symmetry. Ren et al.⁸⁸ obtained a polarization rotation that depends on the intensity of incident light in a chiral metamaterial. Rodrigues et al.⁸⁹ investigated the spectral shift induced by the intensity-dependent refractive index in a structure composed of two perforated silver films. With organic conjugated polymer (PFO), Chen et al.⁸⁴ observed third-harmonic generation CD (THG-CD). The authors also investigated the symmetry selection rules of THG-CD with structures of various symmetries that are coated with PFO.⁹⁰ Recently, Ohnoutek et al.⁹¹ obtained an OA using third-harmonic Rayleigh scattering, which might provide an inspiring piece of insight for nonlinear chiroptical responses. Remarkably, as third-harmonic Rayleigh scattering is an incoherent elastic process, the resulting OA has no linear background, has less requirement on the fundamental frequency, and is compatible with isotropic materials. The same group applied this principle to study semiconductor nanohelices, which allowed for the chiroptical characterization of sample volumes as small as 10^{-5} μL .⁹²

4 Conclusion and Future Prospects

To summarize, we have reviewed the recent advancements in chiral metamaterials with a designated focus on the active and nonlinear aspects. Other than more conventional methods, such as photoexcited carriers, phase-change materials, and electrical doping, we also summarized a relatively new mechanism of the magneto-chiral effect for active tuning. Recent advances have demonstrated significant improvements in the value of the figure of merit for magneto-chiral anisotropy. It would be even more fascinating to find new mechanisms or scenarios that could further increase magneto-chiral anisotropy for practical applications in the chemistry and pharmaceutical fields. Another promising way to achieve active tuning is to reconfigure the structures of chiral metamaterials, for example, using mechanical methods and biochemicals. In addition to directly modulating the chiral metamaterials, the modulation can also occur near the metamaterial using liquid crystals or mechanical membranes. In the nonlinear optical regime, chiral metamaterials are particularly useful for investigating chiroptical properties. We thus also reviewed nonlinear chiral metamaterials based on second and third-order nonlinearities. Interestingly, the third-harmonic Rayleigh scattering OA observed recently is very user-friendly, which may find many applications in identifying nonlinear chiroptical properties in biomedical and chemical species. A summary of the effects observed in this article is shown in Table 1. While the table is not exhaustive, it is meant to guide the reader to relevant literature regarding active-chiroptical mechanisms. In addition, the table outlines several optical effects that have yet to be studied.

The variety of temporally tailorable chiroptic devices continues to grow, and with each active mechanism demonstrated, a new potential application is also realized. For instance, while reconfigurable chiral metamaterials typically do not have the responsivities necessary for information communication or data systems, they have a great deal of potential in sensing for batch or continuous flow reactive systems in both the chemical and pharmaceutical industries. Moreover, incorporating harmonic or nonlinear optics either as surface or bulk mediums has shown to have a great sense of opportunity for providing rapid and highly sensitive analysis of chiral analytes. However, the opportunity for polarization conversion or switching is not limited to the chemical realm; by targeting some of the remaining challenges in this field, the use of chiroptic metamaterials will also impact other applications. As active chiroptical metasurfaces continue to aim for near-lossless polarization conversion, the field will open up incredible opportunities for polarization division multiplexing in analog photonic computing.

One of the challenges for tuning chirality is achieving a high modulation depth or switching the handedness completely at strong CD or OA with low energy consumption. To address this

Table 1 A summary of active optical effects demonstrated in both static and reconfigurable chiral metamaterials with a variety of different activating/transducer mechanisms. The “/” represents an “or.” The table is a broad survey of literature to the best of the authors’ knowledge and should not be considered an exhaustive list.

Inputs	Active mechanism		
	Static	Reconfigurable	To be studied
Optical modulation	Photo-generated carriers ⁴⁵⁻⁴⁷		
	Ultrafast switching ⁹³		
Optical nonlinear	Second harmonic generation ^{83,85,86}		Self-phase modulation
	Third harmonic generation ^{84,90,92}		Sum/difference frequency generation
	Nonlinear OA/self-focusing ^{88,89}		
Thermal	Phase change ⁴⁸⁻⁵⁰	Optothermal ⁷⁷	Thermal-mechanical expansion
Electrical	Electro-optic effect ⁵¹⁻⁵³		Capacitive doping/carrier accumulation
	Electrogyration/electro-optic activity ⁹⁴		Franz–Keldysh
	Optical rectification ⁴²		Electrochromic
Magnetic	Magneto-optic effect ⁵⁴		
	Magneto-chiral dichroism ^{56,57}		
	Transverse magneto-optical Kerr effect		
	Voigt/magneto-electro-optical ⁹⁵		
	Optical gyromagnetic ⁹⁶		
Mechanical		MEMS/NEMS ^{53,60,61,64,65}	Piezooptic effect
		Pneumatic ⁶²	Thermal-mechanical expansion
		Photoelasticity/stretching ^{63,66}	
		Hydrogel absorption ⁶⁷	
		Liquid crystal ^{75,76}	
Chemical/biological		DNA controlled ⁷²	
		Chemical reaction ⁷³	
		Solvents ⁷⁴	
		Photocatalysis ^{98,99}	

challenge, the first step is to create chiral metamaterials that only respond to one selected handedness while being inert to the other. One example is to use spin preserving meta-mirrors with structured metals so that one-handedness of the circularly polarized light has zero reflection.¹⁰⁰ Given the intrinsic material loss of metals, the chirality of the metallic metamaterials is often limited. For an enhanced chirality, Gorkunov et al.¹⁰¹ employed the concept of bound states in the continuum with dielectrics. The tailored resonant metamaterials only couple to one circular polarization of light so that the co-polarized transmission is more than 90%. Fabrication errors and defects cause scattering loss in addition to the material loss. Spin-momentum locked topological photonics immune to scattering loss could thus further enhance the chirality. The second

step is to look for novel materials and structures that efficiently complete the switching process. To that end, some promising candidates are phase change materials and 2D materials.

From the device perspective, creating monolithic devices using chiral metamaterials hybridized with 2D materials can dramatically reduce the device footprints, thus potentially decreasing energy consumption. For example, detecting the full-Stokes polarization of light is vital for many applications but typically demands complex and bulky optical systems. Li et al.¹⁰² achieved this functionality in a monolithic chiral device by integrating chiral metamaterials with graphene. In addition to full-Stokes polarimetry, it would be intriguing to see how hybrid monolithic devices could reach many more functionalities, such as spectral detection and tunable chiral light sources on a chip. Also, 2D materials do not have to be limited to more conventional semimetals, semiconductors, or dielectrics. They can also be 2D ferromagnetic, ferroelectric, and magnetic materials. Therefore, monolithic and hybrid chiral devices are promising for their contributions to valleytronics, spintronics, and chiral quantum optics.

Acknowledgments

S.L. acknowledges the start-up fund from Texas A&M University, including the Governor's University Research Initiative (GURI) fund for the Invent Labs at Texas A&M University. S.L. also acknowledges the T3: Texas A&M Triads for Transformation Fund and the generous endowment by Mr. Holly Frost.

References

1. L. D. Barron, *Molecular Light Scattering and Optical Activity*, 2nd ed., pp. 1–443, Cambridge University Press (2004).
2. N. Berova et al., *Comprehensive Chiroptical Spectroscopy*, Vol. 1, pp. 1–791, John Wiley and Sons (2012).
3. N. Berova, K. Nakanishi, and R. W. Woody, *Circular Dichroism: Principles and Applications*, R. W. Woody and N. Berova Eds., 2nd ed., p. 912, Wiley-VCH (2000).
4. J. Gal, “The discovery of biological enantioselectivity: Louis Pasteur and the fermentation of tartaric acid, 1857—a review and analysis 150 yr later,” *Chirality* **20**(1), 5–19 (2008).
5. K. P. C. Vollhardt and N. E. Schore, *Organic Chemistry: Structure and Function*, W.H. Freeman (2007).
6. D. Adam, “Chemistry prize reflects tailor-made reactions,” *Nature* **413**(6857), 661 (2001).
7. B. List, R. A. Lerner, and C. F. Barbas, “Proline-catalyzed direct asymmetric aldol reactions,” *J. Am. Chem. Soc.* **122**(10), 2395–2396 (2000).
8. K. A. Ahrendt, C. J. Borths, and D. W. C. MacMillan, “New strategies for organic catalysis: the first highly enantioselective organocatalytic diels - Alder reaction,” *J. Am. Chem. Soc.* **122**(17), 4243–4244 (2000).
9. S. Beychok and E. A. Kabat, “Optical activity and conformation of carbohydrates. I. Optical rotatory dispersion studies on immunochemically reactive amino sugars and their glycosides, milk oligosaccharides, oligosaccharides of glucose, and blood group substances,” *Biochemistry* **4**(12), 2565–2574 (1965).
10. A. Rosenberg, “The optical rotatory dispersion of aromatic amino acids and the side chain-dependent cotton effects in proteins,” *J. Biol. Chem.* **241**(21), 5119–5125 (1966).
11. B. Jirgensons, *Optical Activity of Amino Acids, Peptides, and Proteins*, pp. 47–56, Springer, Berlin, Heidelberg (1973).
12. A Correspondent in Molecular Petrology, “Optical activity of proteins,” *Nature* **212**(5069), 1399–1399 (1966).
13. E. Plum et al., “Giant optical gyrotropy due to electromagnetic coupling,” *Appl. Phys. Lett.* **90**(22), 223113 (2007).
14. X. Yin et al., “Interpreting chiral nanophotonic spectra: the plasmonic Born-Kuhn model,” *Nano Lett.* **13**(12), 6238–6243 (2013).
15. M. Hentschel et al., “Three-dimensional chiral plasmonic oligomers,” *Nano Lett.* **12**(5), 2542–2547 (2012).

16. C. Helgert et al., “Chiral metamaterial composed of three-dimensional plasmonic nanostructures,” *Nano Lett.* **11**(10), 4400–4404 (2011).
17. M. Decker, M. Wegener, and S. Linden, “Coupling effects in low-symmetry planar split-ring resonator arrays,” *Opt. Lett.* **34**(10), 1579–1581 (2009).
18. V. K. Valev et al., “Chirality and chiroptical effects in plasmonic nanostructures: fundamentals, recent progress, and outlook,” *Adv. Mater.* **25**(18), 2517–2534 (2013).
19. C. M. Soukoulis and M. Wegener, “Past achievements and future challenges in the development of three-dimensional photonic metamaterials,” *Nat. Photonics* **5**(9), 523–530 (2011).
20. Z. Li, M. Gokkavas, and E. Ozbay, “Manipulation of asymmetric transmission in planar chiral nanostructures by anisotropic loss,” *Adv. Opt. Mater.* **1**(7), 482–488 (2013).
21. W. Gao et al., “Circular dichroism in double-layer metallic crossed-gratings,” *J. Opt.* **13**(11), 115101 (2011).
22. Y. Cui et al., “Giant chiral optical response from a twisted-arc metamaterial,” *Nano Lett.* **14**(2), 1021–1025 (2014).
23. C. Wu et al., “Spectrally selective chiral silicon metasurfaces based on infrared Fano resonances,” *Nat. Commun.* **5**(1), 1–9 (2014).
24. S. P. Rodrigues et al., “Metamaterials enable chiral-selective enhancement of two-photon luminescence from quantum emitters,” *Adv. Mater.* **27**(6), 1124–1130 (2015).
25. E. Hendry et al., “Ultrasensitive detection and characterization of biomolecules using superchiral fields,” *Nat. Nanotechnol.* **5**(11), 783–787 (2010).
26. J. K. Gansel et al., “Gold helix photonic metamaterial as broadband circular polarizer,” *Science (80-.)* **325**(5947), 1513–1515 (2009).
27. M. D. Turner et al., “Miniature chiral beamsplitter based on gyroid photonic crystals,” *Nat. Photonics* **7**(10), 801–805 (2013).
28. Y. Zhao, M. A. Belkin, and A. Alù, “Twisted optical metamaterials for planarized ultrathin broadband circular polarizers,” *Nat. Commun.* **3**(1), 1–7 (2012).
29. W. Cai and V. M. Shalae, *Optical Metamaterials: Fundamentals and Applications*, p. 200, Springer (2009).
30. W. Li et al., “Circularly polarized light detection with hot electrons in chiral plasmonic metamaterials,” *Nat. Commun.* **6**(1), 1–7 (2015).
31. J. C. Bose, “On the rotation of plane of polarisation of electric wave by a twisted structure,” *Proc. R. Soc. Lond.* **63**(389–400), 146–152 (1898).
32. Y. Chen et al., “Multidimensional nanoscopic chiroptics,” *Nat. Rev. Phys.* **2021**, 1–12 (2021).
33. P. Lodahl et al., “Chiral quantum optics,” *Nature* **541**(7638), 473–480 (2017).
34. A. M. Shaltout, V. M. Shalae, and M. L. Brongersma, “Spatiotemporal light control with active metasurfaces,” *Science (80-.)* **364**(6441), eaat3100 (2019).
35. L. Kang, R. P. Jenkins, and D. H. Werner, “Recent progress in active optical metasurfaces,” *Adv. Opt. Mater.* **7**(14), 1801813 (2019).
36. C. A. Emeis, L. J. Oosterhoff, and G. De Vries, “Numerical evaluation of Kramers—Kronig relations,” *Proc. R. Soc. Lond.. Ser. A. Math. Phys. Sci.* **297**(1448), 54–65 (1967).
37. P. L. Polavarapu, “Kramers-Kronig transformation for optical rotatory dispersion studies,” *J. Phys. Chem. A* **109**(32), 7013–7023 (2005).
38. D. K. Hore, A. L. Natansohn, and P. L. Rochon, “Optical anisotropy as a probe of structural order by stokes polarimetry,” *J. Phys. Chem. B* **106**(35), 9004–9012 (2002).
39. N. I. Zheludev, “The road ahead for metamaterials,” *Science (80-.)* **328**(5978), 582–583 (2010).
40. K. Fan and W. J. Padilla, “Dynamic electromagnetic metamaterials,” *Mater. Today* **18**(1), 39–50 (2015).
41. Y. Tang and A. E. Cohen, “Enhanced enantioselectivity in excitation of chiral molecules by superchiral light,” *Science (80-.)* **332**(6027), 333–336 (2011).
42. L. Kang et al., “An active metamaterial platform for chiral responsive optoelectronics,” *Adv. Mater.* **27**(29), 4377–4383 (2015).
43. S. Zhang et al., “Negative refractive index in chiral metamaterials,” *Phys. Rev Lett.* **102**(2), 023901 (2009).

44. M. Hentschel et al., “Chiral plasmonics,” *Sci. Adv.* **3**(5), e1602735. (2017).
45. K. Konishi, M. Kuwata-Gonokami, and N. Kanda, “Light-induced terahertz optical activity,” *Opt. Lett.* **34**(19), 3000–3002 (2009).
46. J. Zhou et al., “Terahertz chiral metamaterials with giant and dynamically tunable optical activity,” *Phys. Rev. B – Condens. Matter Mater. Phys.* **86**(3), 035448 (2012).
47. S. Zhang et al., “Photoinduced handedness switching in terahertz chiral metamolecules,” *Nat. Commun.* **3**(1), 1–7 (2012).
48. X. Yin et al., “Active chiral plasmonics,” *Nano Lett.* **15**(7), 4255–4260 (2015).
49. J. A. Burrow et al., “Chiral phase change nanomaterials,” arXiv:2111.09940 (2021).
50. S. Wang, L. Kang, and D. H. Werner, “Hybrid resonators and highly tunable terahertz metamaterials enabled by vanadium dioxide (VO₂),” *Sci. Rep.s* **7**(1), 1–8 (2017).
51. T. T. Kim et al., “Electrical access to critical coupling of circularly polarized waves in graphene chiral metamaterials,” *Sci. Adv.* **3**(9), e1701377 (2017).
52. S. J. Kindness et al., “A terahertz chiral metamaterial modulator,” *Adv. Opt. Mater.* **8**(21), 2000581 (2020).
53. Z. Shen et al., “Mechanically reconfigurable and electrically tunable active terahertz chiral metamaterials,” *Extrem. Mech. Lett.* **51**, 101562 (2022).
54. H. Mai Luong et al., *Active Ag/Co Composite Chiral Nanohole Arrays*, American Chemical Society (2021).
55. G. L. J. A. Rikken and E. Raupach, “Observation of magneto-chiral dichroism,” *Nature* **390**(6659), 493–494 (1997).
56. G. Armelles et al., “Interaction effects between magnetic and chiral building blocks: a new route for tunable magneto-chiral plasmonic structures,” *ACS Photonics* **2**(9), 1272–1277 (2015).
57. S. Lan et al., “Observation of strong excitonic magneto-chiral anisotropy in twisted bilayer van der Waals crystals,” *Nat. Commun.* **12**(1), 1–7 (2021).
58. J. R. Schaibley et al., “Valleytronics in 2D materials,” *Nat. Rev. Mater.* **1**(11), 1–15 (2016).
59. J. C. W. Song and N. M. Gabor, “Electron quantum metamaterials in van der Waals heterostructures,” *Nat. Nanotechnol.* **13**(11), 986–993 (2018).
60. T. Kan et al., “Enantiomeric switching of chiral metamaterial for terahertz polarization modulation employing vertically deformable MEMS spirals,” *Nat. Commun.* **6**(1), 1–7 (2015).
61. T. Kan et al., “Spiral metamaterial for active tuning of optical activity,” *Appl. Phys. Lett.* **102**(22), 221906 (2013).
62. C. Feng et al., “2D to 3D convertible terahertz chiral metamaterial with integrated pneumatic actuator,” *Opt. Express* **26**(11), 14421–14432 (2018).
63. T. Kosuge et al., “Mechanical large deformation 3D chiral THz metamaterial,” in *Proc. IEEE Int. Conf. Micro Electro Mech. Syst. 2020-January*, IEEE, pp. 1292–1295 (2020).
64. H. Kwon and A. Faraon, “NEMS-tunable dielectric chiral metasurfaces,” *ACS Photonics* **8**, 2980–2986 (2021).
65. S. Chen et al., “Electromechanically reconfigurable optical nano-kirigami,” *Nat. Commun.* **12**(1), 1–8 (2021).
66. H. T. Lin et al., “Optical chirality tunable and reversible plasmonic chiral metasurfaces on flexible PDMS substrate,” in *Conf. Lasers and Electro-Opt., CLEO 2019–Proc.* (2019).
67. Y. Guan et al., “Chiral plasmonic metamaterials with tunable chirality,” *ACS Appl. Mater. Interfaces* **12**, 50192–50202 (2020).
68. B. Ai, H. M. Luong, and Y. Zhao, “Chiral nanohole arrays,” *Nanoscale* **12**(4), 2479–2491 (2020).
69. Y. He et al., “Optimized fan-shaped chiral metamaterial as an ultrathin narrow-band circular polarizer at visible frequencies,” *Nanotechnology* **29**(16), 165301 (2018).
70. G. K. Larsen et al., “The fabrication of three-dimensional plasmonic chiral structures by dynamic shadowing growth,” *Nanoscale* **6**(16), 9467–9476 (2014).
71. P. Moitra et al., “Large-scale all-dielectric metamaterial perfect reflectors,” *ACS Photonics* **2**(6), 692–698 (2015).
72. A. Kuzyk et al., “Reconfigurable 3D plasmonic metamolecules,” *Nat. Mater.* **13**(9), 862–866 (2014).

73. X. Duan et al., “Hydrogen-regulated chiral nanoplasmonics,” *Nano Lett.* **16**(2), 1462–1466 (2016).
74. Z. Wu et al., “High-performance ultrathin active chiral metamaterials,” *ACS Nano* **12**(5), 5030–5041 (2018).
75. B. Wang et al., “Liquid-crystal-loaded chiral metasurfaces for reconfigurable multiband spin-selective light absorption,” *Opt. Express* **26**(19), 25305–25314 (2018).
76. Y. Ji et al., “Active terahertz spin state and optical chirality in liquid crystal chiral metasurface,” *Phys. Rev. Mater.* **5**(8), 085201 (2021).
77. S. Zanutto et al., “Optomechanics of chiral dielectric metasurfaces,” *Adv. Opt. Mater.* **8**(4), 1901507 (2020).
78. P. Fischer and F. Hache, “Nonlinear optical spectroscopy of chiral molecules,” *Chirality* **17**(8), 421–437 (2005).
79. M. A. Belkin and Y. R. Shen, “Non-linear optical spectroscopy as a novel probe for molecular chirality,” *Int. Rev. Phys. Chem.* **24**(2), 257–299 (2007).
80. T. Petralli-Mallow et al., “Circular dichroism spectroscopy at interfaces: a surface second harmonic generation study,” *J. Phys. Chem.* **97**(7), 1383–1388 (2002).
81. T. Verbiest et al., “Strong enhancement of nonlinear optical properties through supramolecular chirality,” *Science (80-.)* **282**(5390), 913–915 (1998).
82. J. T. Collins et al., “Chirality and chiroptical effects in metal nanostructures: fundamentals and current trends,” *Adv. Opt. Mater.* **5**(16), 1700182 (2017).
83. V. K. Valev et al., “Nonlinear superchiral meta-surfaces: tuning chirality and disentangling non-reciprocity at the nanoscale,” *Adv. Mater.* **26**(24), 4074–4081 (2014).
84. S. Chen et al., “Giant nonlinear optical activity of achiral origin in planar metasurfaces with quadratic and cubic nonlinearities,” *Adv. Mater.* **28**(15), 2992–2999 (2016).
85. V. K. Valev et al., “The origin of second harmonic generation hotspots in chiral optical metamaterials [Invited],” *Opt. Mater. Express* **1**(1), 36–45 (2011).
86. S. P. Rodrigues et al., “Nonlinear imaging and spectroscopy of chiral metamaterials,” *Adv. Mater.* **26**(35), 6157–6162 (2014).
87. L. Gui et al., “Nonlinear Born-Kuhn analog for chiral plasmonics,” *ACS Photonics* **6**(12), 3306–3314 (2019).
88. M. Ren et al., “Giant nonlinear optical activity in a plasmonic metamaterial,” *Nat. Commun.* **3**(1), 1–6 (2012).
89. S. P. Rodrigues et al., “Intensity-dependent modulation of optically active signals in a chiral metamaterial,” *Nat. Commun.* **8**, 14602 (2017).
90. S. Chen et al., “Symmetry-selective third-harmonic generation from plasmonic meta-crystals,” *Phys. Rev. Lett.* **113**(3), 033901 (2014).
91. L. Ohnoutek et al., “Optical activity in third-harmonic Rayleigh scattering: a new route for measuring chirality,” *Laser Photonics Rev.* **15**(11), 2100235 (2021).
92. L. Ohnoutek et al., “Third-harmonic Mie scattering from semiconductor nanohelices,” *Nat. Photonics* **2022**, 1–8 (2022).
93. L. Kang et al., “Nonlinear chiral meta-mirrors: enabling technology for ultrafast switching of light polarization,” *Nano Lett.* **20**(3), 2047–2055 (2020).
94. Q. Zhang et al., “Electrogyration in metamaterials: chirality and polarization rotatory power that depend on applied electric field,” *Adv. Opt. Mater.* **9**(4), 2001826 (2021).
95. J. Valente et al., “A magneto-electro-optical effect in a plasmonic nanowire material,” *Nat. Commun.* **6**(1), 1–7 (2015).
96. W. Yang et al., “Observation of optical gyromagnetic properties in a magneto-plasmonic metamaterial,” *Nat. Commun.* **13**, 1719 (2022).
97. Z. Wang et al., “Gyrotropic response in the absence of a bias field,” *Proc. Natl. Acad. Sci. U. S. A.* **109**(33), 13194–13197 (2012).
98. Y. Negrin-Montecelo et al., “Chiral generation of hot carriers for polarization-sensitive plasmonic photocatalysis,” *J. Am. Chem. Soc.* **144**(4), 1663–1671 (2022).
99. L. K. Khorashad et al., “Hot electrons generated in chiral plasmonic nanocrystals as a mechanism for surface photochemistry and chiral growth,” *J. Am. Chem. Soc.* **142**(9), 4193–4205 (2020).

100. L. Kang et al., “Preserving spin states upon reflection: linear and nonlinear responses of a chiral meta-mirror,” *Nano Lett.* **17**(11), 7102–7109 (2017).
101. M. V. Gorkunov et al., “Bound states in the continuum underpin near-lossless maximum chirality in dielectric metasurfaces,” *Adv. Opt. Mater.* **9**(19), 2100797 (2021).
102. L. Li et al., “Monolithic full-stokes near-infrared polarimetry with chiral plasmonic meta-surface integrated graphene-silicon photodetector,” *ACS Nano* **14**(12), 16634–16642 (2020).

Shoufeng Lan is an assistant professor (2009 to present) in Mechanical Engineering (primary) and Materials Science and Engineering (affiliated) at Texas A&M University. He focuses on understanding wave-matter interactions in natural and engineered structures and materials at small scales (micro, nano, molecular, and atomic). Much of his research has built upon three intriguing platforms: metamaterials, plasmonic structures, and two-dimensional (2D) materials.

Biographies of the other authors are not available.